"Non constriction based immobilization of polymer spheres for bio-sensing and scaffold based applications"

Undergraduate Thesis

Presented in partial fulfillment of the requirements for the Bachelor of Science with honors research distinction of The Ohio State University

By

Kinshuk Mitra

The Ohio State University-Biomedical Engineering

Graduating May 5, 2014

Dr. Ronald X. Xu, Dr. Michael F. Tweedle

Abstract

Microfluidic devices have been routinely used to perform multiplexed analysis at proteomic, genomic and cellular levels. Such analysis serves to probe fundamental biological questions as well as provide means for clinical diagnosis. At the proteomic and genomic levels, bead based assays are commonly used as solid phases to immobilize antigens for downstream detection. Functional cellular analysis such as proliferation studies use microbeads as scaffolds for cell culture. A significant majority of assay systems use constriction to immobilize beads while sample is flown through to utilize spatial-coding multiplexing strategies or divert maximal fluid flow through sensor beads. Spatial constriction however, results in non uniform flow of fluid across bead surface and substantially increases shear forces on bead surface. In a high-throughput context these limitations are detrimental in terms of assay reproducibility and flow rate limitation respectively. We demonstrate the use of a sandwiched polycarbonate membrane to trap microbeads in a bi-layer microfluidic chip to perform sandwiched ELISA based detection of murine IgG protein. Using flow-rates of 1 ml/hr we established a fluorescence limit of detection of 2 nanograms/ml. In order to validate the device for multimarker, we successfully detected EpCAM (Epithelial Cell Adhesion Marker) at concentration of 5 nanograms/ml using flow-rates of 1 ml/hr. We also explored the usability of our device for single-cell analysis using MCF-7 breast cancer cells as models for proliferation function analysis. Anti-EpCAM coated beads were used to anchor MCF-7 cells via the

EpCAM receptor and serve as scaffold for cell growth. Beads in the chip supplied with growth media experienced viable cell growth as opposed to none of the beads with fixed cells. Growth was recorded for a maximum of 4 days and followed a sigmoid trend. In short, our study demonstrates the usability of a microfluidic chip with integrated membrane component to immobilize solid phase bead for proteomic biosensing and cell proliferation function analysis. Such assays could provide useful means to provide develop point-of-care diagnostic but also interrogate fundamental biologic questions in pathologies such as cancer.

Acknowledgements

I would like to thank my mentors, Dr. Ronald Xu and Dr. Michael Tweedle for their constant encouragement, access to laboratory resources and guidance whenever things went not according to plan. Further thanks should go to colleagues Brett Geiger for cell culture work and Aaron Maharry for co-designing the AutoCAD masks for lithography. Thanks is also due to Dr. Steve Quake and the microfluidics foundry staff for hosting me over the summer and providing a home to try out several ideas which made this project a success. This work was made possible by NCIIA grant 9872-12 OncoFilter to M.T and K.M. Thanks also to Shu-Wei and Keisha Milum as well as Dr. Shankaran for advice regarding cell biology and conjugation chemistry respectively. Thank you all.

Vita

RESEARCH EXPERIENCE

Microfluidic high purity analyte enrichment; Mentors: Drs. Michael Tweedle, Ronald Xu July 2012-Present

Testing feasibility of fluidic device to enrich and filter rare proteins and plasma from peripheral blood
Iterating system for device architecture optimization: multiplexing and throughput

Microfluidic isolation of PBMCs and plasma from whole blood; PI: Dr. Stephen Quake May 2013-Present

Microfluidic devices to replace Ficoll-Plaque for PBMCs and blood plasma isolation from infants and neonates

GRANTS AND FELLOWSHIPS

- National Collegiate Inventors and Innovators Alliance with the Lemelson Foundation: RFP Grant for
- Circulating tumor cell enrichment device. Role: Lead Grant writer and Project Lead $25K +$50K investment
- Pelotonia Cancer Foundation Undergraduate Fellowship: For Research in rapid detection of circulating tumor cells Role: Lead Grant writer and Project Lead □□
- Engineering Research Fellowship: For invention of devices that mediate human social interactions Role: Lead gggGrant Writer and Project Lead
- The State of Ohio-Honda Education Grant: For the establishment of course and teaching assistantship in teaching creativity and innovation in STEM disciplines Role: Lead Grant writer and Project Lead (50 students/ year).

COMMERCIALIZATION ACTIVITY

- First Place, Ohio State University Deloitte Business Plan competition 2013 and First Place Shark Tank, Rice University Alliance Business Plan Competition 2013.
- CTO, OncoFilter microfluidic genomic and proteomic enrichment chip from whole blood for cancer diagnostics.
- First Undergraduate to be awarded Student Innovator of the Year Award (2013), Ohio State University

PUBLICATIONS AND PATENTS

- Mitra, Kinshuk, et al. "Indocyanine-green-loaded microballoons for biliary imaging in cholecystectomy." *Journal of Biomedical Optics* 17.11 (2012): 116025-116025.
- Mitra, Kinshuk, Christine C. Charyton, and Robert Gustafson. "A Demonstration of a Mastery Goal Driven Learning Environment to Foster Creativity in Engineering Design: Tackling the National Academy of Engineering Grand Challenges." *PLoS One (submitted) Preprint available at SSRN* (2013) *on Google Scholar*.
- U.S Provisional Patent Nos. 61/604,714 and 61/605,981 Ohio State U. Office of Technology Commercialization

PUBLICATIONS IN PROGRESS

Kinshuk Mitra, Brett C. Geiger, Ronald X. Xu, Michael F. Tweedle, "Non constriction based immobilization of polymer spheres for bio-sensing and scaffold based applications"

Kinshuk Mitra, Gino Su, Ismail E Araci, Stephen R Quake "Soft lithography fabrication of trapezoid channels for microfluidic inertial PBMC separation" for *Lab on a Chip*

Fields of Study

Biomedical Engineering

Table of Contents

List of Illustrations

Chapter 1: Introduction

Microfluidic devices have traditionally played important roles in rare sample handling for applications such as sequencing, rare cell isolation, cell sorting and in-vitro diagnostics (1-3). Multimarker panel based diagnostics are especially amenable to microfluidic platforms as the automation dramatically increases throughput while conserving sample and reagent use. Systems biology approaches have delineated the importance of multimarker analysis in discerning pathology state and have significantly increased the efficacy of multimarker panels. Li et al. recently demonstrated a systems biology informed process of marker panel selection using multi-reaction monitoring mass spectrometers as instruments to select for the marker cluster with the highest positive predictive value (4). To implement such tests at feasible costs and viable time spans would require tools at the point-of-care. Bead based assays within microfluidic devices have been extensively reviewed with several platforms undergoing clinical testing for cardiovascular and cancer based pathologies (5,6). A majority of bead based systems utilize constriction to immobilize the solid phase bead while the mobile phase with target analytes is flown over (7-9). While this maximizes analyte-detector interaction and provides a spatial coding system for multiplexing, constriction severely hampers fluid flow across the bead. COMSOL simulations represented in Figure 1below highlights the high shear zones and radial non-uniform flow patterns created in constriction systems. This is primarily the result of the continuity principle as demonstrated in Equation 1 below.

$$V_{initial} * A_{inlet} = V_{final} * A_{outlet} \quad (1)$$

V: Velocity; A: Cross sectional area

Flow introduced at 1 ml/hr along the z-axis resulted in maximal shear of 4.1379 mPa at constriction edges. The shear stress increases as the outlet cross-sectional area is far lower than that of the inlet, therefore necessitating an increase in velocity and as a result, shear stress. These effects can not only selectively over-saturate certain portion of the solid phase and hence hamper detection, but also limits the flow-rates so as to not shear the detection moiety off the bead.

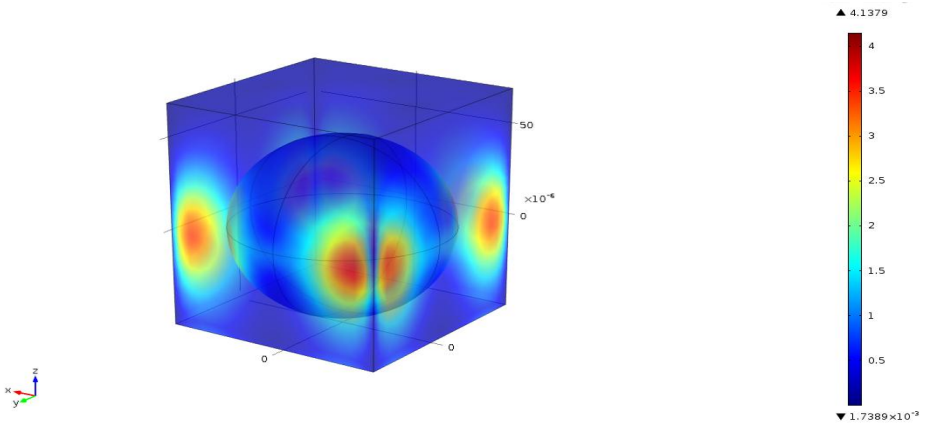

Figure 1. Simulation of shear stress profile along a sensor bead constricted to prevent movement of the solid phase bead. Fluid flow is along the z-axis. High shear stress patterns are observed at corners with no radial symmetry. Regions of beads are overexposed to flow while other regions receive minimal fluid contact.

Systems biology has also emphasized the need for a discrete understanding of biological systems. At the single cell level, assays probing function at levels such as genomic, proteomic and secretomic is proving essential for interrogating immune repertoire, drug discovery, effects of drugs and monitoring immunotherapy (10-13). Functional proliferation assays are important in the oncology context to ascertain combination therapies that can overcome the clonal diversity of tumors. Rather than testing combination therapies on patients followed by RECIST-MRI evaluation, single cells may be individually assessed for resistance to drug or induced phenotypic/genotypic change under pharmacologic pressure. Should such functional measurements be performed via bulk cellular analysis, signal averaging could result in loss of information of information from a crucial minority sub-population. Figure 2 below highlights this challenge. Simply, if heterogeneous cell population (different colors) is sampled in bulk, the result only indicates an average representation of the population versus the single cell analysis platform which completely captures the diversity in the population.

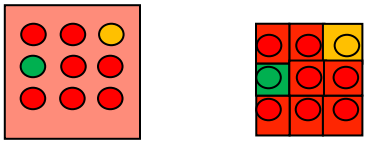

(A) (B)

Figure 2. In case A function measurement of heterogeneous cell (marked with different colored circles) at the bulk level captures an average signal without providing information on the level and kind of population heterogeneity. In case B single cell analysis provides information on both the type and level of population heterogeneity.

In this thesis, we outlay a device with capability to perform multimarker detection without constriction to retain the solid phase. We also exploit the radial uniform flow across the solid phase to utilize the said phase as a scaffold for single cell proliferation assays. We hypothesized that a bi-layer microfluidic device with a polycarbonate membrane in the middle can effectively trap solid phase beads for sandwich ELISA based quantification of biomarkers. Two independent protein analytes, murine IgG and human EpCAM were used on chip, producing calibration curves and to ascertain limits of detection. Fluorescent readout along the region of interest (solid bead) was obtained by pixel by pixel intensity readout to produce a score that was associated for a given concentration of antigen. Finally, to ascertain the capability of our microfluidic device to function as a micro bio-reactor, we introduced single MCF-7 breast cancer cells onto chip. Chips were infused with standard culture media for four days and growth was recorded via Live/Dead membrane dyes (Life Technologies, CA).

The fact that both multimarker immunoassays and single cell assays can be performed on the same chip also lends to another important note. Multimarker immunoassays are vital as each marker component has a role to play at the systems level. A holistic comprehension of the states of the different components enables a detailed understanding of the state of the system and consequently state of pathology. Cells also execute function based on their states and function as components of a system. These two distinct categories of components, one at the microscale and another at the nanoscale, function cooperatively within both healthy and diseased tissues. Devices that can provide

functionalities that bridge across such wide physical scales may provide unique information as to the interaction of these different categories of components and their states in the context of such interactions.

Chapter 2: Device Fabrication

The microfluidic device named as the OncoFilter, uses standard soft lithography techniques to create microfluidic channels on Polydimethylsiloxane (PDMS). Briefly, transparency masks were constructed using designs constructed on AutoCAD (Autodesk Inc., CA). Masks were utilized to produce silicon molds using optical contact lithography (Stanford Microfluidics Foundy, CA). Sylgard-184 PDMS (Dow Corning, MI) was poured over silicon mold at a 10:1 ratio between PDMS and cross linking agent. After degassing, molds were baked at 70 degree Celsius in ovens for 2 hours. To bond dual layers of PDMS chip with the 12 micron pore polycarbonate membrane (Whatman, NJ), an APTES enhanced reactive oxygen plasma mediated bonding strategy was used. Aran et. al. detailed such a strategy previously and utilized similar device to separate plasma from whole blood (14). A detailed schematic of a single channel of our chip is depicted in Figure 3 below.

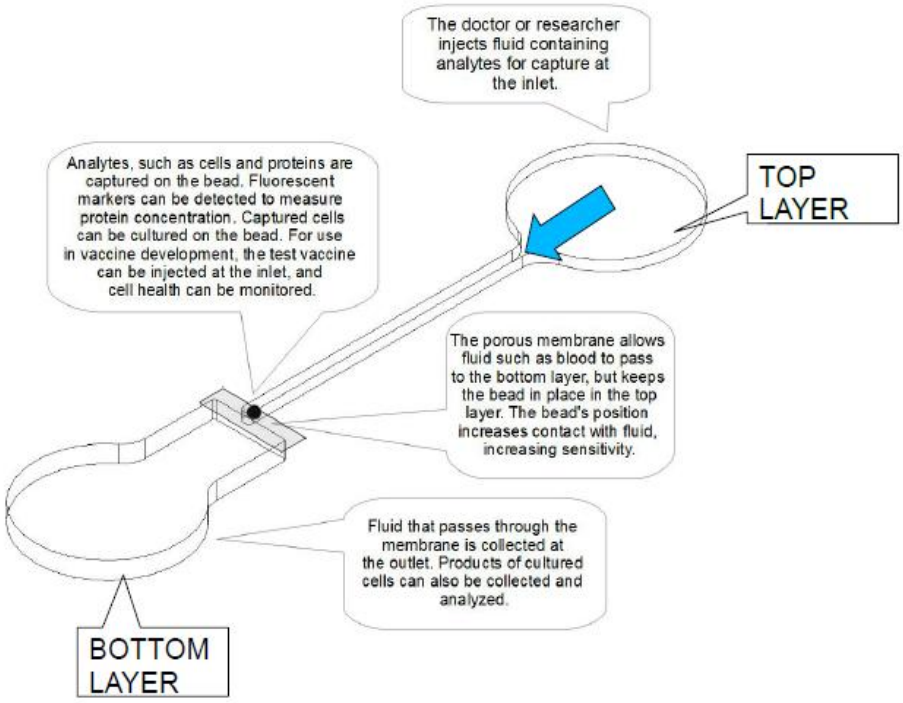

Figure 3. A single channel of the OncoFilter device. Multiple such channels are arrayed in parallel on a single device. Blue arrow indicates the direction of fluid flow.

As can be seen from the COMSOL simulation in Figure 4, the OncoFilter bead based system also enables directing maximal flow of sample through the sensor bead enhancing contact with target analytes.

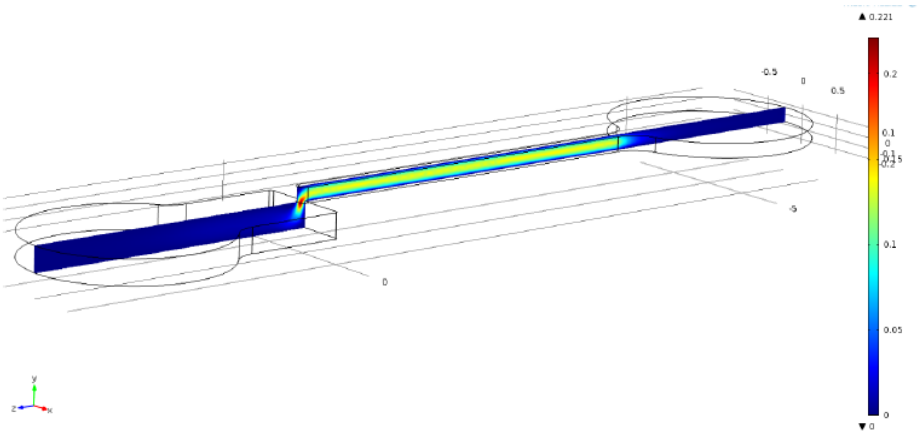

Figure 4. COMSOL simulation of flow through single channel of device. Fluidic flow is maximally through the point of overlap between two fluidic layers. Point of overlap is also position of the sensor bead. Flow within channel was under constant observation of optical microscope (Olympus, PA). Standard plastic tubing and 18 gauge needles were used to interface microfluidic channels with macroscopic flow systems. Luer-lock syringes were used as sample dispensing units with controlled release using syringe pump.

COMSOL simulations were also undertaken to probe the benefit of using polycarbonate membranes instead of constriction. Figure 5 shows the fluidic shear stress of beads within channels.

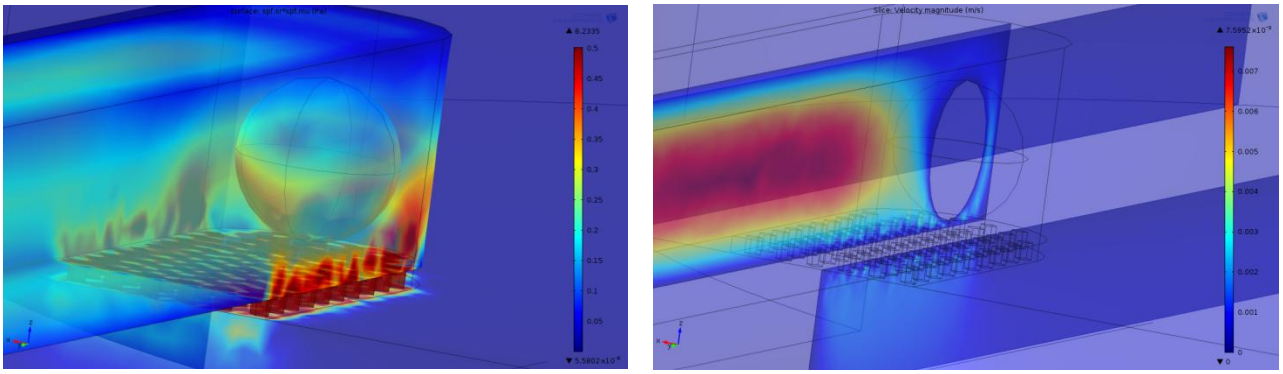

(a) (b)

Figure 5. COMSOL simulation of the (a) shear stress experienced by beads under a 1ml/hr flow rate and (b) velocity flow profile. Membrane is placed directly under the bead and modeled using porosity information obtained from manufacturer.

Polystyrene beads (mean 100 micron) with high polydispersity (>99%) and surface functionalized with strepavidin was purchased from Spherotech Inc. Beads were conjugated with desired antibodies, either anti-EpCAM (Abcam, MA) or anti-IgG (Sigma Aldrich, MO) according to manufacturers instruction. Single beads were isolated using micropipette and optical microscope and introduced into the microfluidic chip via the inlet and application of negative pressure. Figure 6 depicts a sensor bead trapped within the overlap region of the top and bottom flow layers in the microfluidic chip.

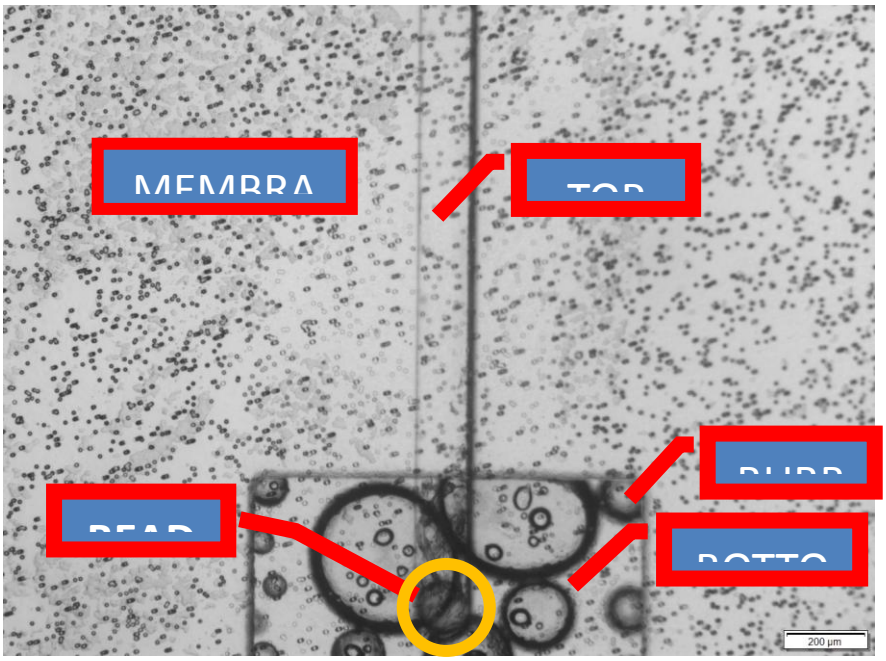

Figure 6. Sensor bead (circled in yellow) trapped within the microfluidic channel by the membrane. Bubbles can be removed by subjecting the system to a greater duration of flow and thus infusing the entire chip with fluid.

Chapter 3: Demonstration of functional capabilities of device

Antigen model EpCAM and murine IgG were utilized to demonstrate microfluidic sandwich the ELISA on the OncoFilter. Detection was performed using fluorescence secondary detection antibody using FITC fluorophore for IgG and IR-800 for EpCAM respectively. Prior to testing, the device was infused with bovine serum albumin and incubated for 30 minutes. To obtain a calibration curve, antigen was diluted in 1 milliliter phosphate buffered saline (pH 7.4) at predetermined concentrations. Flow was introduced into the chip at 1ml/hr for 1 hour. Each chip housed five sensor beads, three which were exposed to flow and served as replicates, two which were unexposed to flow and served as controls. Each chip was flushed with PBS at 3ml/hr for 30 minutes. Figure 7 highlights the sensing capability of the OncoFilter towards a 28 kilodalton protein, EpCAM. EpCAM was detected using a secondary detection antibody conjugated with IR-800 CW dye.

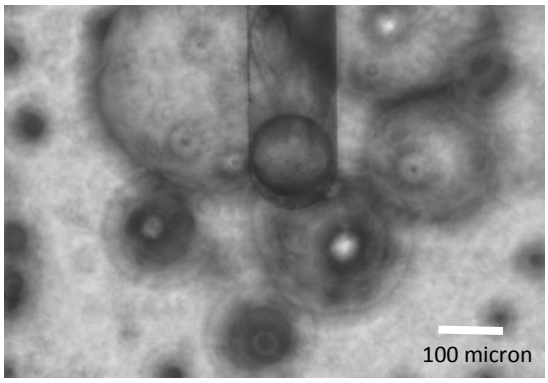

(a)

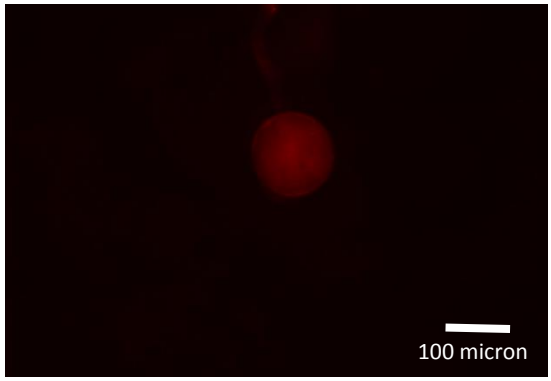

(b)

Figure 7. Imaging of the trapped bead. (a) Bead trapped over the overlap region and over the membrane within the chip. Bead is conjugated with anti-EpCAM. (b) After infusion of EpCAM and secondary anti-EpCAM conjugated with IR-800 CW, chip is imaged under fluorescence microscope with IR 800 filter.

Intensity readout was performed using homebrew image analysis system. Greyscale images of both sides of sensor beads were obtained via fluorescent microscope. Pixel by pixel intensity was calculated into a cumulative fluorescence score. Maximum fluorescence concentration readout limit was set at 10ng/ml for EpCAM. All subsequent measured fluorescence was normalized to the maximum limit intensity. The calibration curve obtained was plotted in Figure 8 below. The curve was found to be consistent to the expected log-linear trend.

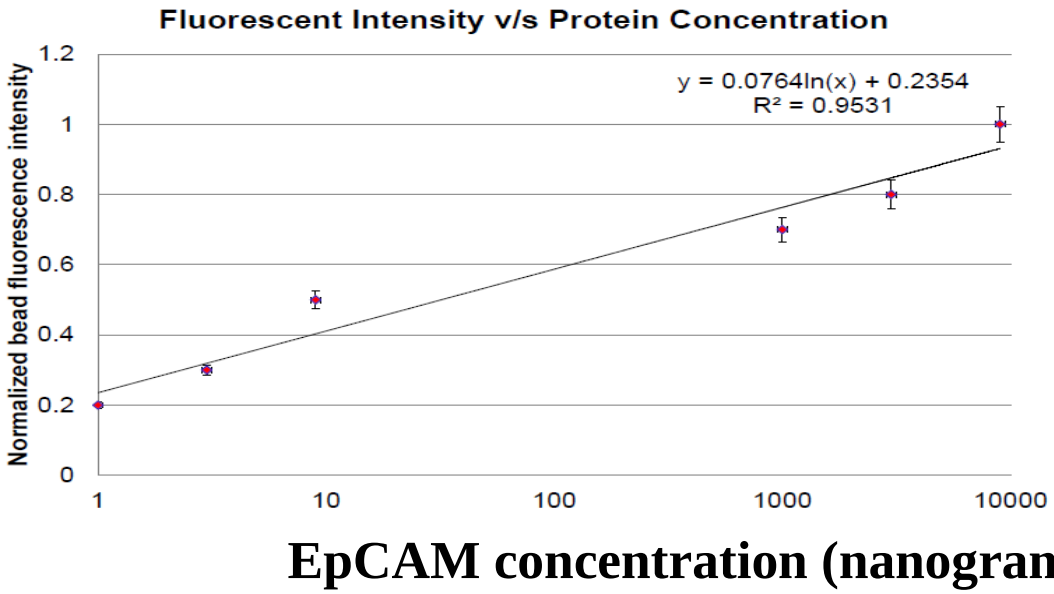

Figure 8. Calibration curve for varying EpCAM concentrations. Curve is plotted against fluorescence intensity of the bead measured by CCD imaging. Intensity readings are normalized to the fluorescence measurement obtained at 10,000 ng/ml.

To ensure the OncoFilter system was capable of detecting multiple markers, detection tests were run using murine IgG. Due to the constraint on time and the lack of need to validate the quantitative power of the device, calibration curve experiments were not performed. Qualitative comparison of FITC based detection of murine IgG to the IR-800 based detection of EpCAM is depicted in Figure 9 below.

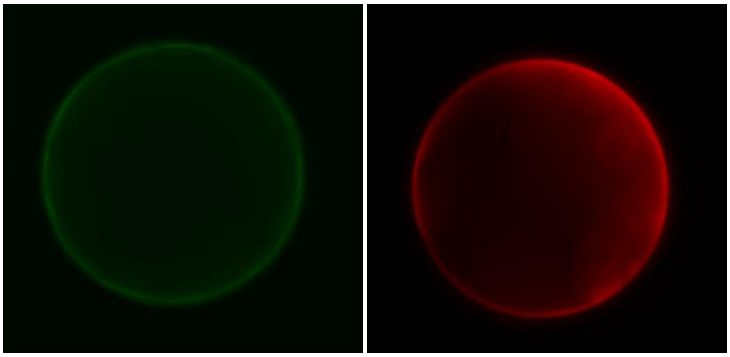

Figure 9. Sensor beads that detects IgG using FITC (green) and EpCAM using IR-800 (red). Both sensor beads experienced uniform radial exposure to the antigen. Antigen exposure was maximal at bead margins. The higher quantum yield of FITC is evidenced by the slight background scatter around the bead. Comparatively, the IR-800 bead enjoys a higher signal-to-noise ratio though IR-800 dyes enjoy significantly lower fluorescent quantum yields.

We hypothesized that because of the non-constriction based radially uniform flow, the OncoFilter could function as a bioprocessor. Bead based microfluidic devices generally make poor bioreactors as constriction leads to non-uniform flow across the bead. To ascertain this functionality, beads were coated with anti-EpCAM and loaded onto the chip. EpCAM expressing MCF-7 cells were singly separated using a micropipette and loaded onto the chip. In order to maintain uniform conditions, all five available channels of a device were loaded with single beads, either as controls with fixed cells or for experiment with live cells. Single MCF-7 cells were inserted until at least one attached to the bead. Over a period of 4 days, beads were infused with media at 10 microliter/hr and imaged once at 0, 24 and 96 hours. Figure 10 below depicts the fluorescent capture of the bead-cell culture system and Figure 11 plots the progression of cell growth over the 4 day period.

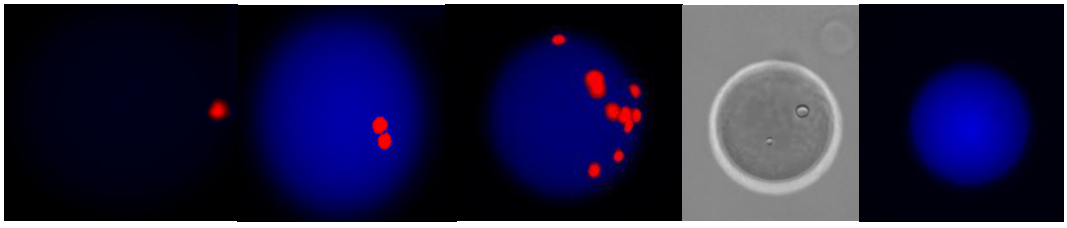

0hrs 24hrs 96hrs Controls with 2 cells

Figure 10. Growth of cells on bead over the course of 4 days. Bead experienced slight rotation and movement during perfusion. Red cells were live and were the only ones counted. Control bead with 2 cells was fixed and observed no growth.

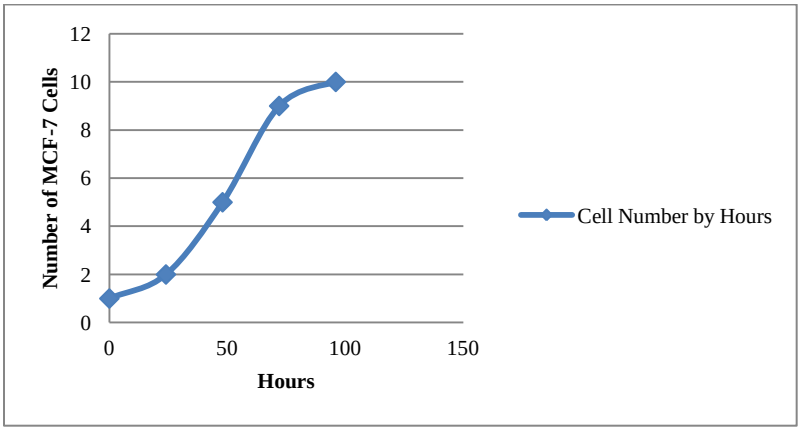

Figure 11. Plotting the growth of a single cell in OncoFilter. Growth of single cell on bead scaffold over time followed the sigmoid trend. Fresh media was inserted into the dispensing tube daily.

Chapter 4: Discussion and Conclusion

We investigated the capability of a membrane trapped bead based microfluidic device to perform proteomic sensing and cell culture. As membranes allow for non-constriction based capture of bead, protein detection and quantification was carried out by a modified sandwich ELISA protocol on-chip. In the absence of constriction, the shear stress experienced by the portion of the bead facing the flow and therefore under maximum exposure, was minimal compared to the side of the bead facing the wall of the conduit and therefore, constricted. This can be attributed to the navier-stokes equation under the case of low Reynold's number. Under such conditions, flow follows path of least resistance with excess flow exiting the conduit via the membrane. This reduces fluidic velocity on the surface of the bead proximal to the entrance as expected from the flow continuity equations. In all models flow was expressed as incompressible with a no-slip boundary condition. The capability of such a device to perform quantitative protein sensing was validated by the use of human EpCAM as a model antigen. Secondary antibody conjugated to IR-800 dye was used as a quantitative fluorescent marker imaged using inverted fluorescent microscopy as can be seen in Figure 7. Calibration curve experiments were conducted to determine, a limit of detection and a correlation function between fluorescent intensity and antigen concentration produced results comparable to values and trends reported in literature (15, 16). We obtained a limit of detection at 10 ng/ml for EpCAM and a log-linear calibration curve. The sample consisting of 100 ng/ml of murine IgG was detected using secondary antibody conjugated to FITC on chip by

application of protocol used to detect EpCAM. As Figure 9 demonstrated, both use of FITC and IR-800 was feasible and similar in the formation of a brighter fluorescent ring along the outline of the bead. This could potentially be due to the planar imaging of a spherical bead which would increase the concentration of signal around the periphery. We also observed sigmoid cell growth trend in Figure 11 when culturing MCF-7 cells. This is expected as cell doubling time decreases and cell growth reaches a point of saturation as competition for nutrients increases.

A major limitation of our device as evidenced by the flow velocity simulation in Figure 5b is the absence of contact between a bulk of our sample and the bead. While the non-constriction strategy we employed did reduce shear stress, it also reduced opportunity for interaction between antigen in sample and capture antibodies on the bead. Moving forward, COMSOL simulations such as those in Figure 12 would guide the design of devices that use height to redirect flow entirely past the bead while retaining the non-constriction principles employed in our original designs. As the simulations demonstrate, this would still ensure extremely low shear rates, uniform flow coverage and maximum juinteraction between analytes and the bead.

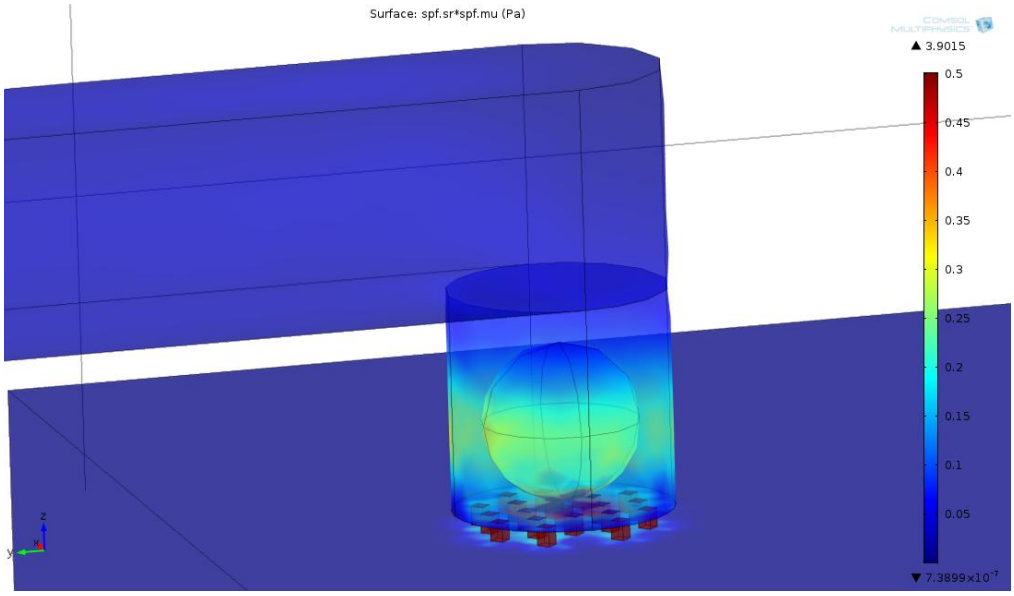
Surface: spf.sr*spf.mu (Pa)
▲ 3.9015
0.5
0.45
0.4
0.35
0.3
0.25
0.2
0.15
0.1
0.05
▼ 7.3899×10⁻⁷

(a)

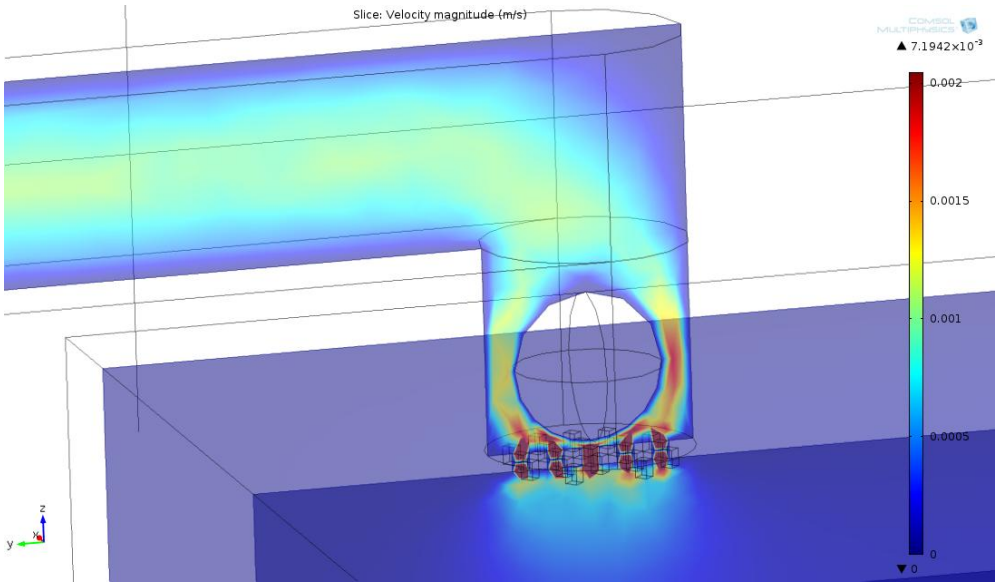
Slice: Velocity magnitude (m/s)
▲ 7.1942×10⁻³
0.002
0.0015
0.001
0.0005
0
▼ 0

(b)

Figure 12. COMSOL simulations of future designs (a) The shear stress on the bead is much better radially distributed through the use of a cylindrical cavity (b) The flow velocity simulation demonstrates that the bead is maximally exposed to the sample.

In conclusion, our experiments demonstrate the advantages of using a non-constriction type immobilized bead-based assay to perform immunoassays under lower shear stress and with better fluidic distribution around the bead. We characterize and demonstrate a functional model capable of performing quantitative sandwich ELISA as well as serve as a micro-bioreactor. Future experiments will build on our proof of principle to construct chips where the bead is placed directly in the path of a straight fluid flow ensuring maximal exposure to sample.

Chapter 5: References

1. Ottesen, Elizabeth A., et al. "Microfluidic digital PCR enables multigene analysis of individual environmental bacteria." *Science* 314.5804 (2006): 1464-1467.
2. Ozkumur, Emre, et al. "Inertial Focusing for Tumor Antigen–Dependent and–Independent Sorting of Rare Circulating Tumor Cells." *Science translational medicine* 5.179 (2013): 179ra47-179ra47.
3. Ma, Chao, et al. "A clinical microchip for evaluation of single immune cells reveals high functional heterogeneity in phenotypically similar T cells." *Nature medicine* 17.6 (2011): 738-743.
4. Li, Xiao-jun, et al. "A blood-based proteomic classifier for the molecular characterization of pulmonary nodules." *Science translational medicine* 5.207 (2013): 207ra142-207ra142.
5. Chou, Jie, et al. "Hot embossed polyethylene through-hole chips for bead-based microfluidicdevices." *Biosensors and Bioelectronics* 42 (2013): 653-660.
6. Raamanathan, Archana, et al. "Programmable bio-nano-chip systems for serum CA125 quantification: toward ovarian cancer diagnostics at the point-of-care."*Cancer Prevention Research* 5.5 (2012): 706-716.
7. Jokerst, J. V., Chou, J., Camp, J. P., Wong, J., Lennart, A., Pollard, A. A., ... & McDevitt, J. T. (2011). Location of Biomarkers and Reagents within Agarose Beads of a Programmable Bio-nano-chip. *Small*, *7*(5), 613-624.

8. Zhang, Qing, et al. "Microbial detection in microfluidic devices through dual staining of quantum dots-labeled immunoassay and RNA hybridization."*Analytica chimica acta* 556.1 (2006): 171-177.

9. Erickson, David, and Dongqing Li. "Integrated microfluidic devices." *Analytica Chimica Acta* 507.1 (2004): 11-26.

10. Georgiou, George, et al. "The promise and challenge of high-throughput sequencing of the antibody repertoire." *Nature biotechnology* (2014).

11. Weaver, Westbrook M., and Robert Damoiseaux. "Single-Cell Microfluidic Cytometry for Next-Generation High-Throughput Biology and Drug Discovery."*Cell-Based Microarrays*. Springer New York, 2014. 75-96.

12. Mach, Albert J., Oladunni B. Adeyiga, and Dino Di Carlo. "Microfluidic sample preparation for diagnostic cytopathology." *Lab on a Chip* 13.6 (2013): 1011-1026.

13. Wei, Wei, et al. "Microchip platforms for multiplex single-cell functional proteomics with applications to immunology and cancer research." *Genome Biology* 14 (2013): R94.

14. Aran, Kiana, et al. "Irreversible, direct bonding of nanoporous polymer membranes to PDMS or glass microdevices." *Lab on a Chip* 10.5 (2010): 548-552.

15. Tarn, Mark D., and Nicole Pamme. "Microfluidic platforms for performing surface-based clinical assays." (2011): 711-720.

16. Haeberle, Stefan, and Roland Zengerle. "Microfluidic platforms for lab-on-a-chip applications." *Lab on a Chip* 7.9 (2007): 1094-1110.